Crystallization Kinetics of Poly(propylene terephthalate) Studied by Rapid-Scanning Raman Spectroscopy and FT-IR Spectroscopy

Bernard J. Bulkin,*† Menachem Lewin,‡ and Jongsoo Kim§

Department of Chemistry, Polytechnic Institute of New York, Brooklyn, New York 11201.
Received July 16, 1986

ABSTRACT: Vibrational spectroscopy is used to study the crystallization kinetics of poly(propylene terephthalate). Low-frequency Raman spectra of PPT are presented for the first time. While the overall kinetic parameters observed are similar to those for PET, the larger number of conformations available to PPT lead to a distinctive behavior in the early stages of annealing, which can be seen most clearly by following the carbonyl stretching vibration.

Introduction

Poly(propylene terephthalate) (PPT) is the first in the series of aromatic polyesters which has an odd number of methylene groups. The physical properties of PPT are much different from those of the better known even-numbered homologues, poly(ethylene terephthalate) (PET) and poly(butylene terephthalate).

X-ray crystallographic studies of PPT show that the unit cell contains two monomer units and the conformation of the carbon–carbon bonds at the methylene groups is all gauche (GG).[1,2] By contrast, PET has one monomer unit in the unit cell, and the conformation of the methylene groups is trans (T). Certain differences in physical properties might be explained in terms of the difference in conformation. Thermal analysis data on PPT have been obtained by Smith et al.,[3] who determine a T_g of 35 °C and a crystalline melting temperature T_m of 227 °C.

The molecular mobility of the methylene carbons of the aromatic polyesters was studied by ^{13}C NMR spectroscopy.[4] The results of this study are that the terephthaloyl residue is more mobile than the methylene groups for both PET and PPT.

Infrared and Raman spectroscopic studies of PPT, along with the assignment of some bands, were done by Ward et al.[5] as part of a study on the polyester homologues. They also studied the mechanical properties and structure of the fibers of PPT.[6] The recovery and shrinkage behavior of PPT fiber was found to be the best among the aromatic polyester fibers studied. They concluded that the molecular conformation in both the crystalline and amorphous regions plays a key role in determining the mechanical behavior.

To our knowledge, there are no literature reports on the crystallization kinetics of PPT, despite its potential importance both in the fundamental and practical senses. In this paper we report the results of a study of the crystallization kinetics of PPT studied by rapid-scanning Raman spectroscopy and FT-IR spectroscopy. The usefulness of applying vibrational spectroscopy to investigate the crystallization kinetics of polymers has been previously discussed by us.[7,8] The Raman spectrum of PPT in the low-frequency region (<200 cm^{-1}) is also presented for the first time.

Experimental Section

PPT samples in the form of pellets (4 × 4 × 2 mm) were supplied to us (courtesy of Prof. Ryozo Kitamaru, Department of Polymer Chemistry, Kyoto University). The intrinsic viscosity was 0.78 dL/g at 25 °C. The density of the as-received sample was 1.3117 g/mL, indicating a highly amorphous sample. These samples were used, as recieved, for the Raman spectroscopic studies.

Free-standing films for FT-IR spectra were prepared by spreading a small amount of 3% PPT solution in dichloroacetic acid on a glass slide, then applying a slight vacuum (100–150 Torr) at room temperature. Under these conditions, the solvent evaporated very slowly, leaving cloudy crystalline films. To render these films amorphous, they were heated to the melt above 250 °C and held there for 10 min under a nitrogen atmosphere. They were then quenched into liquid nitrogen. The resulting transparent films were peeled off the glass surface in distilled water. The films were dried and stored in a desiccator for at least 1 week at room temperature before use.

Raman data were obtained as described previously.[7] All conditions for annealing were as presented in previous publications.

The FT-IR spectra were obtained with a Digilab FTS 20B spectrometer. Survey spectra were obtained at room temperature at 2-cm^{-1} resolution. For kinetic studies as a function of temperature, a Perkin-Elmer heatable sample holder was used to hold the free-standing films. Digilab GC/IR software was applied to acquire and reduce the spectra in the very short time intervals required.

While signal-to-noise ratios for all spectra were quite high and the data reduced from the spectra for kinetic plots are relatively smooth, there are nonetheless considerable uncertainties in the kinetic parameters derived from these data. In the case of the Avrami equation approach, these uncertainties derive from insufficient data in the short-time region, which has a big effect on the Avrami parameters derived. In the case of the zero-order kinetics, the uncertainty derives from the somewhat arbitrary choice of the straight-line region used.

The density of the annealed samples and the original sample were measured in a Tecam density gradient column DC-1 at 23 °C. A carbon tetrachloride/*n*-heptane mixture was used as the suspending medium.

Results and Discussion

Figure 1 shows Raman spectra in the 500–1800-cm^{-1} region for amorphous and crystalline samples of PPT. Several changes in the spectrum can be observed. First, the band at 1717 cm^{-1} becomes narrower on annealing. When the band is examined carefully, its asymmetry is also found to change, an observation that has been discussed in some detail in a previous paper.[9] Second, a group of bands in the 1400-cm^{-1} region change in a complex way. Ring and diol modes appear in this region, and there is band overlap. Details of these changes were discussed by other authors.[5] Third, a new band appears at 1220 cm^{-1}. While this band seems to be associated with crystallinity, its origin is not clear. It will be shown later that the intensity ratio of this band to that of a band at 1174 cm^{-1} has a linear correlation with density. Fourth, the band at 1115 cm^{-1} changes in a complex fashion. In the case of PET the well-known 1096 cm^{-1} band appears in this region. Finally, there are changes in the 800–960 cm^{-1} region, where both diol and ring modes are found. It appears that

† Present address: Standard Oil Research and Development Co., Cleveland, OH 44128.

‡ Visiting professor. Permanent address: Israel Fiber Institute, Jerusalem, Israel.

§ Partial fulfillment of the requirements for the Ph.D. degree for Jongsoo Kim, Polytechnic Institute of New York, 1986.

0024-9297/87/2220-0830$01.50/0

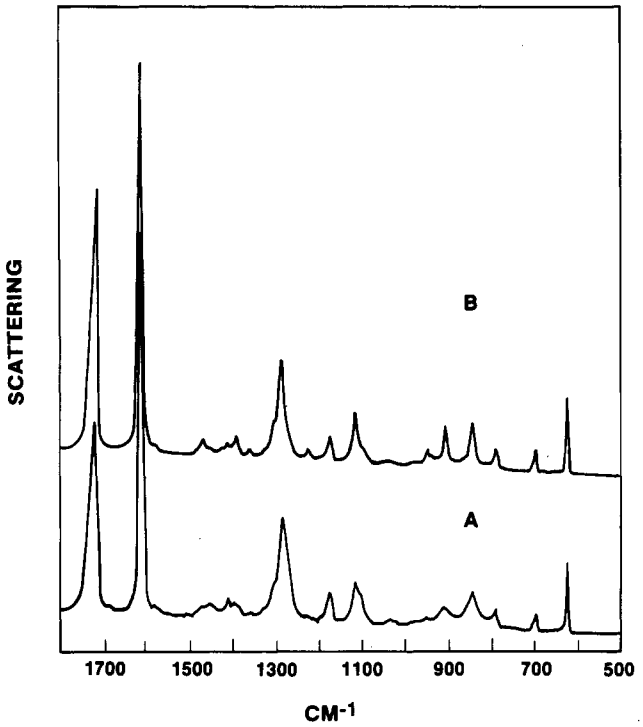

Figure 1. Raman spectra of PPT: (a) amorphous sample; (b) crystalline sample made by annealing for 4 h at 150 °C.

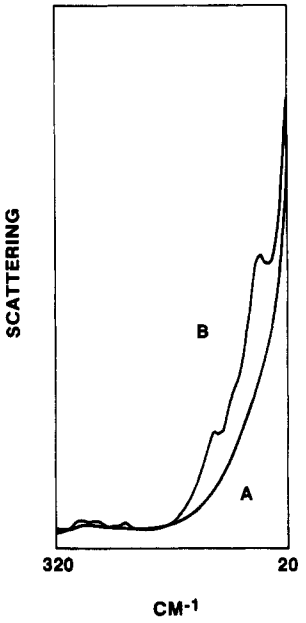

Figure 2. Raman spectra of PPT in the low-frequency region: (a) amorphous sample; (b) crystalline sample made as in Figure 1.

bands at 1610, 1284, and 1174 cm^{-1} do not change upon annealing.

Figure 2 is the first report of the low-frequency Raman spectrum of PPT (20–320 cm^{-1}). The general features of the spectrum are similar to those of PET, presented in a previous publication.[10] Prominent bands at 58, 114, and 287 cm^{-1} appear in crystalline samples, which might correspond to 73, 129, and 273 cm^{-1} in PET. PPT also shows bands at 264 and 228 cm^{-1} and a weak band at 92 cm^{-1}. The spectrum of the amorphous sample is featureless below 150 cm^{-1}.

Figure 3 shows the infrared spectra for amorphous and crystalline PPT in the 600–1600-cm^{-1} region. Close examination of the spectra reveals that the 1409-cm^{-1} band

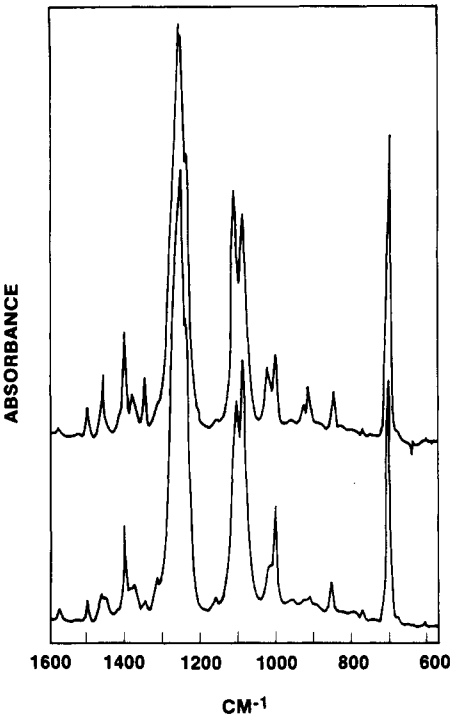

Figure 3. FT-IR spectra of PPT: uppper trace, crystalline sample; lower trace, amorphous sample.

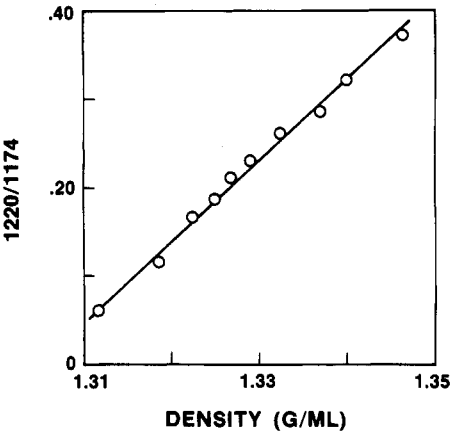

Figure 4. External correlation between 1220/1174-cm^{-1} intensity ratio and density for several annealed samples.

is fairly stable and all other bands appear to change upon annealing. Among the markedly changing bands, those showing increasing intensity at 1358, 1468, 1034, and 933 cm^{-1} were assigned as diol modes, while the decreasing band at 1018 cm^{-1} was assigned as a ring mode. Details of the changes in the spectra and assignments can be found in the literature.[5] These five varying bands, with the 1409-cm^{-1} band as a reference, will be used in the studies of the crystallization kinetics.

The intensity ratio of the 1220-cm^{-1} Raman band to that at 1174 cm^{-1} shows a linear correlation with density, as shown for several samples in Figure 4. As discussed in detail previously,[9] the full width at half-maximum of the carbonyl stretching vibration of PPT does not correlate with density for a range of samples with different crystallinity, while that of PET does. The lower frequency side width at half maximum intensity was found to correlate linearly with density, however.[9]

It is necessary to correct kinetic data, which will be taken as a function of temperature, for the dependence of the carbonyl half-width on temperature which occurs independent of degree of crystallinity. To determine the ap-

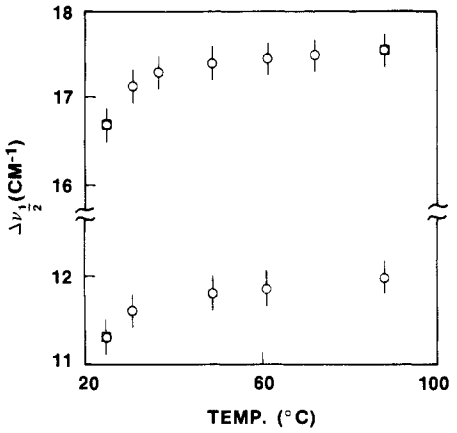

Figure 5. Temperature dependence of carbonyl band half-width for semicrystalline samples: lower curve, sample annealed for 2 h at 150 °C; upper curve, sample annealed for 2 h at 200 °C.

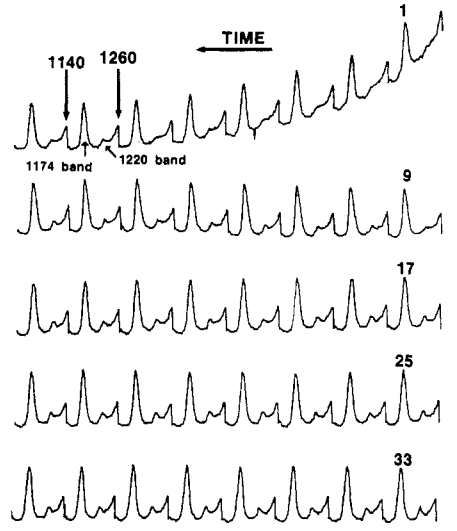

Figure 6. Rapid Raman spectroscopic data in the region 1140–1260 cm^{-1}. Forty scans of the region are shown, with the lower wavenumber to the left in each scan. The beginning and end of scan 7 are marked on the figure, as are the positions of the 1174- and 1220-cm^{-1} bands in this particular scan. For conditions, see text. The growth of the 1220-cm^{-1} band is seen as annealing proceeds at 65 °C.

propriate correction, the temperature dependence of the carbonyl band half-width for crystalline samples was studied. Results are shown in Figure 5. For the upper curve, representing a sample annealed for 2 h at 150 °C, the carbonyl half-width increased from 16.7 cm^{-1} at 25 °C to 17.5 cm^{-1} at 88 °C. When the sample was cooled to 25 °C, the half-width returned to its original value. This point obtained on cooling is marked as a square in the figure. The same result was obtained on the lower curve in the figure, a sample made by annealing for 2 h at 200 °C.

Results on a series of rapid Raman scans of the 1140–1260-cm^{-1} region are shown in Figure 6. In this experiment, annealing was carried out at 65 °C and each scan took 45 s. Under these conditions, there is a very short induction time, following which a new band at 1220 cm^{-1} grows in. The ratio of the intensity of the 1200-cm^{-1} band to that at 1174 cm^{-1} is plotted in Figure 7. The curve looks like well-established crystallization curves for polymers.[11]

With these data, an Avrami plot of the 65 °C annealing experiment can be constructed,[11] with the results shown in Figure 8. The Avrami n value derived from these data is 1.62. Table I gives Avrami n and k values for a series of rapid Raman data in this region. The lack of an induction time at 71 °C makes establishment of an n value

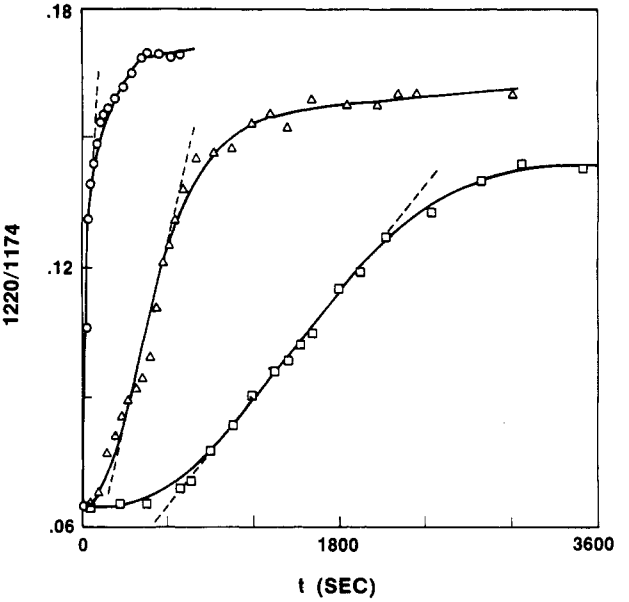

Figure 7. 1220/1174-cm^{-1} intensity ratio vs. time. Data taken from experiments such as Figure 6. Temperatures are 59, 65, and 71 °C. Dotted lines are used for zero-order kinetic analysis.

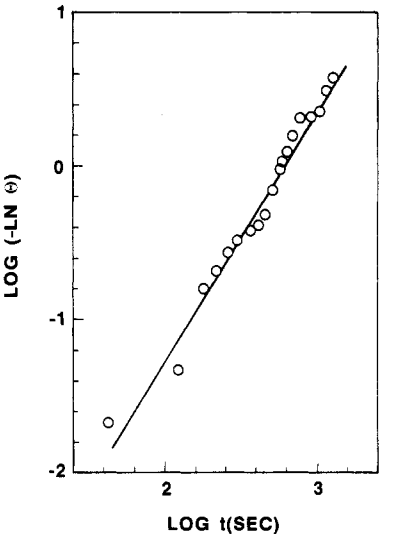

Figure 8. Avrami plot of data from Figure 7, 65 °C.

Table I
Kinetic Parameters Derived from Rapid Raman Spectroscopic Data of 1220/1174-cm^{-1} Ratio

T, °C	Avrami n	Avrami log k	zero-order $k' \times 10^4$, s^{-1}	E_a, kcal/mol
59	1.86	−5.77	0.38	
65	1.62	−4.50	1.14	42.9
71	*a*	−3.84	3.71	

[a] Too rapid to obtain n value.

very uncertain. Similar n values (2 or slightly less than 2) have been reported for PET, probably indicating a similar crystallization mechanism.

In order to get some idea of the activation energy for the process, the initial rapidly growing region is approximated as a straight line (dotted lines in Figure 7). This zero-order approximation gives a rate constant k' that is the slope of the line. Table I summarizes these k' values. An Arrhenius plot yields an activation energy of 43 kcal/mol, similar to that reported from Raman data on PET.[7]

Rapid Raman data have also been obtained on the carbonyl band. As reported previously,[9] with annealing

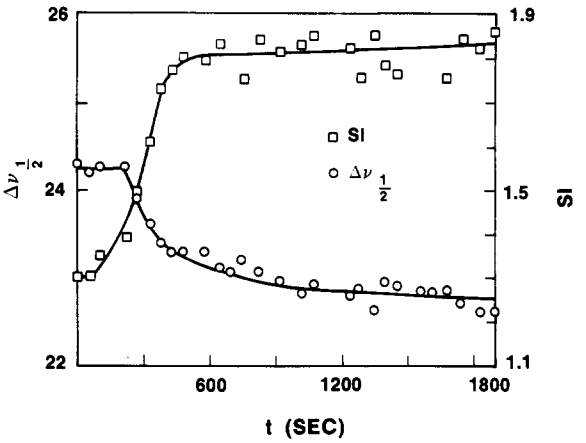

Figure 9. Symmetry index and full-width at half-maximum vs. time for the carbonyl band during annealing at 65 °C.

Table II
Avrami Parameters Derived from Rapid Raman Spectroscopic Data in the 1717-cm^{-1} Region

T, °C	n	log k
66	1.86	−4.65
71	1.53	−3.13

the band becomes unsymmetrical. This may be characterized in terms of a higher frequency site half-width (B) and a lower frequency side half-width (A), or by the symmetry index SI = B/A, in addition to the full-width at half-maximum intensity. These parameters are plotted as a function of time in Figure 9. In the earlier time period, where the overall carbonyl band half-width does not change, the symmetry of the band as seen by SI already begins to change. Since the lower frequency side width (A) was found to correlate linearly with density, Avrami analysis of the data based on A has been done and is shown in Figure 10.

Table II summarizes the data for the transition viewed from the carbonyl group. The n and k values are similar to those of the 1220/1174-cm^{-1} ratio, which means that the overall course of the crystallization is similar.

Figure 11 shows a set of difference IR spectra in the 600–1600-cm^{-1} region, in which the change of the spectra as crystallization proceeds can be easily seen. In the specific experiment shown, annealing was carried out at 78 °C and each scan took 6.25 s. The changes of the intensity of the bands at 1358, 1468, 1034, 933, and 1018 cm^{-1} are observable from the figure. The small increase of the 1409-cm^{-1} band seems to be from the increase in density during crystallization and from contraction of the films. The relative increase in intensity of this band is less than 4%. Using this band as an internal reference band is thus an effective way of correcting the infrared intensity measurements for changes in film thickness.

One object of this research is to check whether there is any difference in crystallization kinetics between various vibrational modes. In fact, the results show that the kinetic behavior of all the glycol modes is similar, while the data on the ring mode (1018 cm^{-1}) was too scattered to give

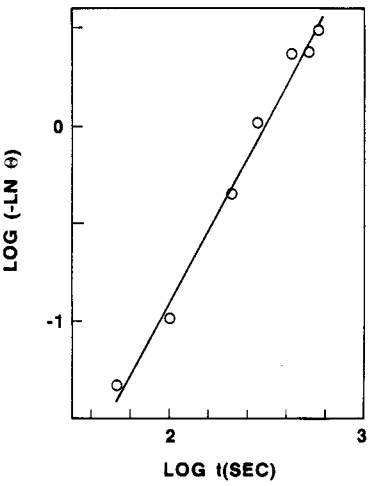

Figure 10. Avrami plot of the lower frequency side of carbonyl half-band-width kinetic data.

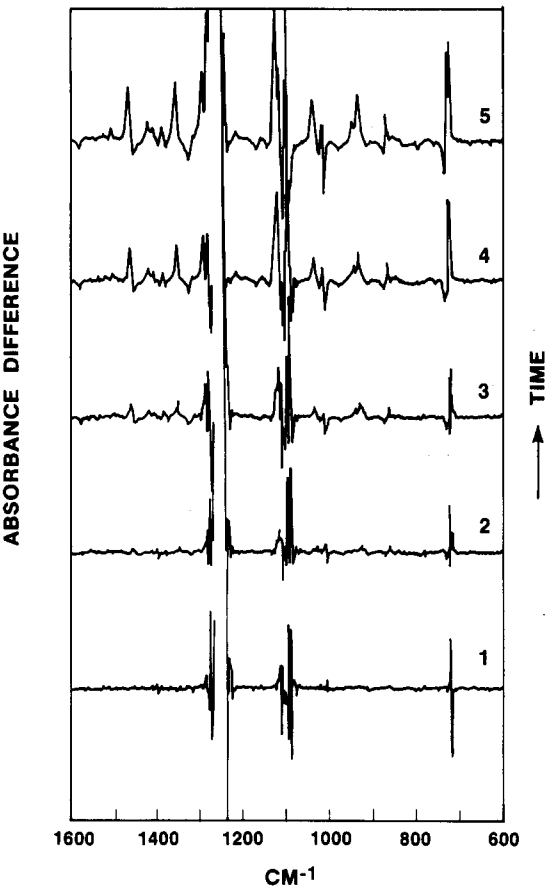

Figure 11. Difference IR spectra in the region 600–1600 cm^{-1}, showing the change of spectra as crystallization proceeds at 78 °C. Time interval between the spectra is 6.3 s.

reliable results. Therefore, in the following section, we will treat only the 1358-cm^{-1} band as typical, with the results on other bands being shown in Table III.

The change of the 1358/1409-cm^{-1} infrared intensity ratio with time was studied at several different tempera-

Table III
Avrami Parameters Derived from the IR Spectroscopic Data

	1358 cm^{-1}		1468 cm^{-1}		933 cm^{-1}		1034 cm^{-1}		1018 cm^{-1}	
T, °C	n	log k	n	log k	n	log k	n	log k	n	log k
58	1.51	−4.41	1.56	−4.54	1.60	−4.59	1.59	−4.57	1.24	−3.54
65	1.66	−4.01	1.84	−4.47	1.86	−4.41	1.82	−4.43	1.87	−4.47
72	1.84	−3.51	1.84	−3.43	1.69	−3.21	1.87	−3.59	1.76	−3.25
78	1.87	−3.05	1.94	−3.17	1.83	−2.98	1.94	−3.14	1.68	−2.52

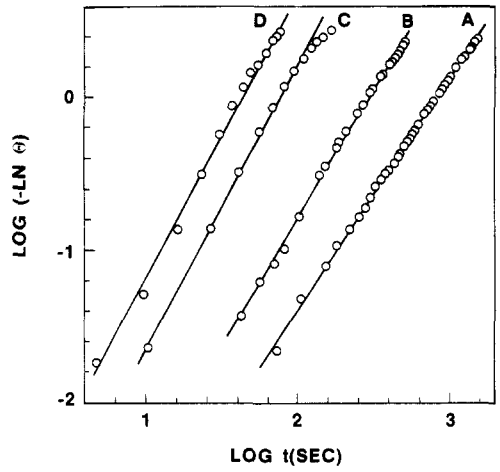

Figure 12. Avrami plots of infrared kinetic data on the 1358-cm^{-1} band: (A) 58 °C; (B) 65 °C; (C) 72 °C; (D) 78 °C.

Table IV
Induction Times (t_i) and Activation Energies Derived from t_i for Changes in the 1358/1409-cm^{-1} Intensity Ratio

T, °C	t_i, s	E_a, kcal/mol
58	135	
65	39	41.2
72	12	
78	6	

tures. Similar results to the Raman data on the 1220/1174-cm^{-1} ratio were obtained. This is to be expected, as both intensity ratios correlate well with density.

To test whether Avrami kinetics can be applied, the data were reduced as shown in Figure 12. Excellent Avrami plots, summarized in Table III, showing single-stage kinetics, are observed. Avrami n values are between 1.6 and 1.9, consistent with Raman data.

An induction time was calculated by extrapolation from the infrared data, and these are tabulated in Table IV. With the assumption that the induction time is inversely proportional to a rate, an activation energy may be derived from this. The Arrhenius plot of these times yields a value of 41.2 kcal/mol. Activation energy for the crystallization may also be calculated, as before, from zero-order rate constants derived from the slopes. These are tabulated for all infrared data in Table V. These rate constants yield activation energies of 40 ± 2 kcal/mol. These values are similar to those reported for PET crystallization.

As the annealing temperature is raised, it can be seen from both infrared and Raman data that the maximum amount of crystallinity increases. If one calculates the plateau value for these data (Figure 13) similar increases are found for both infrared and Raman data. From a thermodynamic equilibrium point of view, higher temperatures should mean lower crystallinity. Therefore, the results must be interpreted in a kinetic framework. It is likely that the higher degrees of crystallinity are related to overcoming barriers to chain disentanglement. Similar effects were noted in PET crystallization.[7]

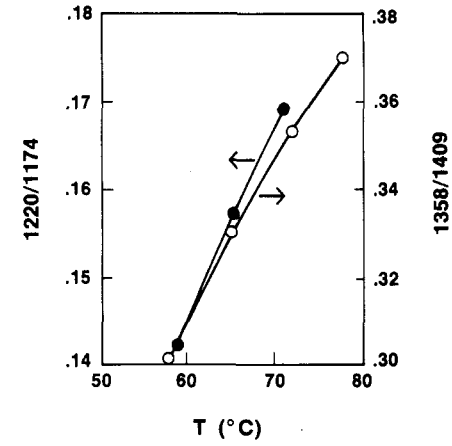

Figure 13. Plot of maximum Raman 1220/1174-cm^{-1} and IR 1358/1409-cm^{-1} band intensity ratios attainable during primary crystallization as a function of temperature. See text for the definition of maximum intensity ratio.

Conclusions

One view of the crystallization process in PET is that of conformational change, including both the transition from gauche and trans amorphous to trans crystalline about the ethylene linkage and rotation of the carbonyl groups from a distribution of nonplanar conformations into a trans planar arrangement. A proof of this view comes from the behavior of the Raman-active 1174-cm^{-1} band. This band, assigned as the totally symmetric A_g ring C–H in-plane bending mode should be infrared inactive for a centrosymmetric system. The appearance of this band in the infrared spectrum of amorphous PET and its concommitant decrease in intensity upon annealing is viewed as confirmation of this view.

The same arguments can be applied in the case of PPT, where the 1173-cm^{-1} band in the infrared spectrum decreases in intensity by 40% upon annealing. Similar behavior is noted for the symmetric ring mode at 1612 cm^{-1}. Thus it is concluded that the motion of the carbonyl groups with respect to the ring is similar in PET and PPT. It is reasonable to expect that this aspect of the crystallization is not affected by the additional methylene group.

The clearest distinction between PET and PPT in the conformational reorganization process comes when the annealing is viewed from the carbonyl band half-width. In the initial stage of the PPT crystallization, there is a reorganization among several conformers, affecting their relative population distribution. However, the number of conformers populated neither increases nor decreases appreciably, as the full width is unchanged. During this same period there is significant change in the density and in the population of new conformers as viewed from the 1220/1174-cm^{-1} intensity ratio.

This difference between PET and PPT can be explained in terms of the crystal packing and crystal structure. For PET, the all-trans planar conformation is the most effective in packing chains, and its formation always leads to an increase in density. In the case of PPT, the most

Table V
Zero-Order Rate Constants (k', s^{-1}) and Activation Energies (E_a) Derived from These Constants for the Several IR Bands

	1358 cm^{-1}		1468 cm^{-1}		1034 cm^{-1}		1018 cm^{-1}		933 cm^{-1}	
T, °C	$10^4k'$	E_a	$10^4k'$	E_a	$10^4k'$	E_a	$10^4k'$	E_a	$10^4k'$	E_a
58	1.62		1.23		0.97		2.35		1.12	
65	5.83		4.53		3.42		3.70		4.22	
		40.8		39.1		40.1		37.5		39.3
72	19.96		17.04		13.83		21.98		15.60	
78	55.14		45.44		29.01		49.60		31.93	

stable conformation, TGGT, is not the only one that is available to reduce density from the amorphous material. We conclude that since, on annealing, the crystal structure of PPT assumes a nonplanar helix-like structure, the difference in conformation of the methylene groups leads to little difference in the effectiveness of close packing of the chains. During the conformational reorganization of the initial state, other less stable conformations such as GTTG also appear to help the chains pack, resulting in an increase in density. The density of crystalline PET, 1.46 g/mL, is significantly higher than that of PPT, 1.39 g/mL.

Acknowledgment. This work was supported by the Polymers Program of the National Science Foundation, Grant DMR-8304220. We thank Dr. R. Kitamaru for the sample of PPT.

Registry No. PPT (SRU), 9022-20-2; PPT (copolymer), 25610-17-7.

References and Notes

(1) Dandurand, S. P.; Perez, S.; Revol, J. R.; Brisse, F. *Polymer* **1979**, *20*, 419.
(2) Desborough, I. J.; Hall, I. H.; Neisser, J. Z. *Polymer* **1979**, *20*, 545.
(3) Smith, J.; Kibler, C.; Sublett, B. *J. Polym. Sci, Part A-1* **1966**, *4*, 1851.
(4) Horii, F.; Hirai, A.; Murayama, K.; Suzuki, T.; Kitamaru, R. *Macromolecules* **1983**, *16*, 273.
(5) Ward, I. M.; Wilding, M. A. *Polymer* **1977**, *18*, 327.
(6) Ward, I. M.; Wilding, M. A.; Brody, H. *J. Polym. Sci., Polym. Phys. Ed.* **1976**, *14*, 263.
(7) Bulkin, B. J.; Lewin, M.; McKelvy, M. L. *Spectrochim. Acta, Part A* **1985**, *41A*, 251.
(8) Bulkin, B. J.; Lewin, M.; DeBlase, F. J. *Macromolecules* **1985**, *18*, 2587.
(9) Kim, J. S.; Lewin, M.; Bulkin, B. J. *J. Polym. Sci., Polym. Phys. Ed.*, in press.
(10) DeBlase, F. J.; McKelvey, M. L.; Lewin, M.; Bulkin, B. J. *J. Polym. Sci., Polym. Lett. Ed.* **1985**, *23*, 109.
(11) Schultz, J. *Polymer Materials Science*; Prentice-Hall: Englewood Cliffs, NJ, 1974.
(12) See, for example: Mandelkern, L. *Crystallization of Polymers*, McGraw-Hill: New York, 1964.

Kinetic Model for Tensile Deformation of Polymers. 1. Effect of Molecular Weight

Yves Termonia* and Paul Smith†

Central Research and Development Department, Experimental Station, E. I. du Pont de Nemours and Company, Inc., Wilmington, Delaware 19898. *Received July 28, 1986*

ABSTRACT: A new comprehensive kinetic model for the tensile deformation of solid, flexible polymers is presented. The model, which is based on the Eyring chemical activation rate theory, explicity takes into account the role of the weak attractive forces between chains as well as chain slippage through entanglements. Stress–strain curves calculated for melt-crystallized polyethylene are in quantitative agreement with experiment.

Deformation of solid polymers is a very complex subject of great technological and theoretical interest. A number of models have been proposed to describe the various phenomena that may occur during deformation, such as brittle fracture, yielding, strain hardening, etc.[1-5] Most models are, however, only phenomenological or semiquantitative, static representations, which are incapable of providing a unified description of the various morphological changes that may occur depending on the dynamics and on the structure at the molecular level. Here we present a new comprehensive kinetic model for tensile deformation of solid, flexible polymers. The model, which is based on the Eyring activation rate theory,[6] explicitly takes into account the role of the weak attractive forces between chains as well as chain slippage through entanglements. Stress–strain curves calculated for melt-crystallized polyethylene are in quantitative agreement with experiment. The model also reveals the wide variety of morphological changes that may occur during tensile deformation of polymers.

The undeformed (isotropic) polymer solid is represented by a dense network of coiled, entangled macromolecules (Figure 1). Note that no details of the crystallites in the solid are specified.[7] We start with the regular array of entanglements depicted in Figure 1b. The molecular weight between entanglements is independent of the chain length;[8] i.e., the number of entanglements per macromolecule increases linearly with its length. The network is elongated at constant rate $\dot{\epsilon}$ and at temperature T along the y axis. This causes straining of the weak van der Waals (vdW) bonds, which break, according to the kinetic theory of fracture,[9] at a rate

$$\upsilon = \tau \exp[-(U - \beta\sigma)/kT] \quad (1)$$

In eq 1, τ is the thermal vibration frequency, and U and β are respectively the activation energy and volume. σ is the local stress: $\sigma = K\epsilon$, where ϵ is the local strain and K is the elastic constant of the bond. The breaking of the vdW bonds along a chain strand between two entanglements leads to a transfer of the external load to the now effectively isolated chain strand. As the load increases upon further deformation, slippage of that chain through entanglements sets in. It is assumed[4-6] that this occurs at a rate that has the same functional form as that of the vdW bond breakings (eq 1), but with different values for the activation energy U and the activation volume β. Now, σ represents the difference in stress in the two strands of a chain separated by an entanglement. In order to estimate that stress, we turn to the classical theory of rubber elasticity.[4] According to this theory, the stress on a chain strand having a vector length r is

$$\sigma = \alpha\, kT\mathcal{L}^{-1}(r/nl) \quad (2)$$

where n is the number of statistical chain segments and

† Present address: Materials Program and Department of Chemical and Nuclear Engineering, University of California, Santa Barbara, CA 93106.

0024-9297/87/2220-0835$01.50/0